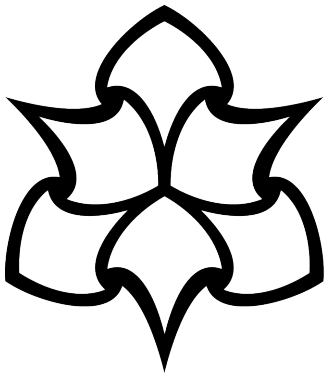

Journal of Molecular and Cellular Cardiology 111 (2017) 86–95

Contents lists available at ScienceDirect

Journal of Molecular and Cellular Cardiology

journal homepage: www.elsevier.com/locate/yjmcc

In-silico investigations of the functional impact of *KCNA5* mutations on atrial mechanical dynamics

Haibo Ni [a], Ismail Adeniran [a], Henggui Zhang [a,b,c,d,*]

[a] Biological Physics Group, School of Physics and Astronomy, The University of Manchester, Manchester, UK
[b] School of Computer Science and Technology, Harbin Institute of Technology, Harbin, China
[c] Space Institute of Southern China, Shenzhen, China
[d] Key Laboratory of Medical Electrophysiology, Ministry of Education, Collaborative Innovation Center for Prevention and Treatment of Cardiovascular Disease/Institute of Cardiovascular Research, Southwest Medical University, Luzhou 646000, China

ARTICLE INFO

Article history:
Received 7 April 2017
Received in revised form 19 July 2017
Accepted 4 August 2017
Available online 10 August 2017

Keywords:
Atrial
KCNA5 mutations
Electromechanical coupling
Atrial contraction
Computer simulation

ABSTRACT

A recent study has identified six novel genetic variations (D322H, E48G, A305T, D469E, Y155C, P488S) in KCNA5 (encoding Kv1.5 which carries the atrial-specific ultra-rapid delayed rectifier current, I_{Kur}) in patients with early onset of lone atrial fibrillation. These mutations are distinctive, resulting in either gain-of-function (D322H, E48G, A305T) or loss-of-function (D469E, Y155C, P488S) of I_{Kur} channels. Though affecting potassium channels, they may modulate the cellular active force and therefore atrial mechanical functions, which remains to be elucidated. The present study aimed to assess the inotropic effects of the identified six KCNA5 mutations on the human atria. Multiscale electromechanical models of the human atria were used to investigate the impact of the six KCNA5 mutations on atrial contractile functions. It was shown that the gain-of-function mutations reduced active contractile force primarily through decreasing the calcium transient (CaT) *via* a reduction in the L-type calcium current (I_{CaL}) as a secondary effect of modulated action potential, whereas the loss-of-function mutations mediated positive inotropic effects by increased CaT *via* enhancing the reverse mode of the Na^+/Ca^{2+} exchanger. The 3D atrial electromechanical coupled model predicted different functional impacts of the KCN5A mutation variants on atrial mechanical contraction by either reducing or increasing atrial output, which is associated with the gain-of-function mutations or loss-of-function mutations in KCNA5, respectively. This study adds insights to the functional impact of KCNA5 mutations in modulating atrial contractile functions.

1. Introduction

The ultra-rapid rectifier delayed potassium channel current, I_{Kur}, is atrial specific and plays an important role in modulating atrial repolarisation as well as contractility [1,2]. Malfunction of the channel disrupts normal cardiac repolarization, resulting in various cardiac rhythm disorders including atrial fibrillation (AF, [3,4]) - the most common sustained cardiac arrhythmia causing morbidity and even mortality [5].

A recent study has identified six novel genetic variations of the KCNA5 gene (D322H, E48G, A305T, D469E, Y155C, P488S) encoding Kv1.5 channels carrying I_{Kur} in patients with early-onset of lone atrial fibrillation (AF) [6]. These mutations produced different modulations on I_{Kur} channel properties, which can be classified into two different groups, the first (D322H, E48G, A305T) resulting in a gain-of-function, and the other (D469E, Y155C, P488S) resulting in loss-of-function of the I_{Kur} channel. By using multi-scale models of the human atria, the pro-arrhythmogenic effects of these genetic variants have been studied, revealing the causative link between the gene mutations and disturbed electrical excitation in the human atria [7]. The difference and similarity between the two groups in their arrhythmogenesis were also investigated [7].

The malfunction of the I_{Kur} channel may also affect atrial contraction, which plays an important role in the overall function of the heart [8–11]. Previous studies have shown that blocking I_{Kur} in the human atrial myocardium led to an elevation of the plateau potential of the action potential (AP) and an increase in the active force development [1,2]. As the identified six gene mutations have profound effects in modulating atrial AP repolarisation phase, causing marked action potential duration (APD) abbreviation or prolongation [7], it is hypothesised that they may impair atrial active force generation in the cells through excitation-contraction coupling, and consequentially affect atrial contractile function. However, the functional inotropic effects of the KCNA5 mutations have not been elucidated, neither have the possible similarities and differences between the two distinctive mutation groups. As altered mechanical contraction in the atria may also affect the electrical activity

* Corresponding author at: Biological Physics Group, School of Physics and Astronomy, The University of Manchester, Manchester, UK.
E-mail address: henggui.zhang@manchester.ac.uk (H. Zhang).

http://dx.doi.org/10.1016/j.yjmcc.2017.08.005

in the myocardium through mechano-electrical feedback (MEF) [12], it is necessary to take MEF into consideration in multi-scale atrial models when evaluating the functional impacts of the KCN5A mutations on atrial electro-mechanical dynamics.

Due to the lack of accurate animal models for KCN5A mutations, computational modelling provides a valuable approach in assessing the functional consequences of electrophysiological alterations on the electro-mechanical dynamics of the heart [13–15]. The aim of this study was to investigate the functional impacts of the KCNA5 variants on the electro-mechanical dynamics of the human atria using multiscale electro-mechanical models.

2. Methods

Descriptions of the methods are detailed in the Online Supplement, and briefed as follows.

2.1. Modelling electromechanical dynamics of human atrial myocytes

Electromechanical models for human atrial cells simulating the electromechanical dynamics of the atrial myocytes were developed in our previous study [16]. Briefly, the Colman et al. model of human atrial electrophysiology [7] was coupled to a modified Rice et al. model of myofilament dynamics [17] and the stretch activated current (I_{SAC}) representing the effect of MEF, resulting in an electromechanical model capable of modelling the time courses of the AP and active force development of atrial myocytes.

To simulate the effect of the KCNA5 mutations on atrial electro-mechanics, the I_{Kur} models developed in a previous study [7] were incorporated into the electromechanical model for WT and KCN5A variants; three mutations (D322H, E48G, A305T) mediating a gain-of-function and three mutations (Y155C, D469E, P488S) resulting in a loss-of-function in I_{Kur}.

To further elucidate the general role of I_{Kur} in modulating the contractility of atrial myocytes, parameters of I_{Kur} channel properties including the channel maximal conductance, the slope ($K_{Activation}$) and half-activation voltage ($V_{1/2}$) of the steady-state activation curve, and time constants of activation and deactivation ($\tau_{Activation}$) were varied over parameter spaces that are within physiologically relevant ranges. More detailed methods on the single cell electrometrical model and parameter analysis are given in Online Supplement 1.1.

2.2. Family of heterogeneous electromechanical models of human atrial myocytes

The atria are electrically heterogeneous with intrinsic differences in their cellular electrophysiological properties across different regions [18,19]. Such electrical heterogeneity has been incorporated extensively in previous modelling studies [14,20–22]. In the present study, the parameters used for the family of regional single cell models in [7] were implemented to simulate the regional electrical heterogeneities in the human atria. Details are given in Online Supplement 1.2.

2.3. 3D anatomical model of electromechanical dynamics

A recently developed anatomically accurate, 3D atrial model of electromechanical coupling for the human atria [14] was updated and implemented to evaluate the inotropic effects of these mutations at the organ level. The 3D electro-mechanical model of human atria (Supplement Fig. 1) was described in detail in [14] and is briefly introduced in Online Supplement 1.3.

2.4. Numerical methods

Numerical methods implemented in the present study are introduced in Online Supplement 1.4.

3. Results

3.1. The inotropic effects of the KCNA5 mutations on atrial myocytes

The inotropic effects of KCNA5 mutations on cellular (right atrial (RA) cell model) electromechanical dynamics are shown in Fig. 1. Compared to WT condition, the mutations modulated the AP dynamics (Fig. 1Ai & Aii), leading to altered calcium transient (CaT) of atrial myocytes (Fig. 1Bi & Bii). As a consequence, marked changes in the active force production (Fig. 1Ci & Cii) and SL shortening (Fig. 1Di & Dii) were observed.

However, there are marked differences in the functional impact between the gain- and loss-of-function mutation groups. The gain-of-function mutations abbreviated APD (except D322H, which prolonged APD but suppressed plateau AP), and reduced the amplitude of CaT, leading to a pronounced decrease in the active force of the myocytes: the maximum active force was reduced by 22.0%, 13.2% and 23.0% for D322H, E48G and A305T vs. the WT conditions, respectively (Fig. 1Ci). Consequently, the impaired contractile force resulted in more significant changes to the sarcomere length (SL) shortening: the relative SL

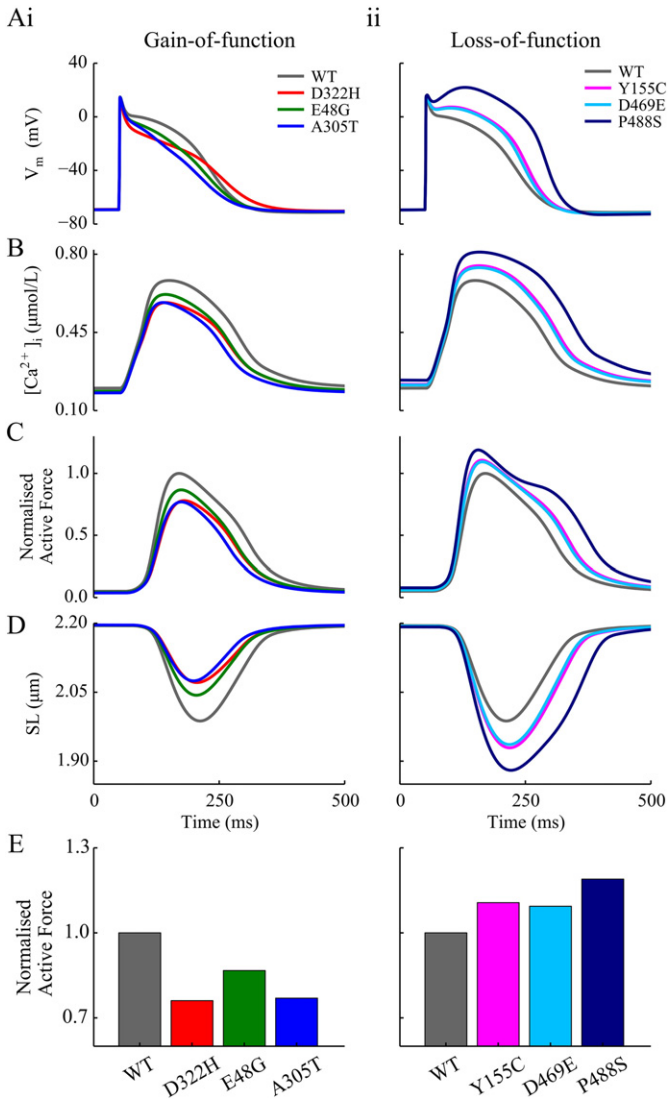

Fig. 1. Simulated inotropic effects of KCNA5 mutations on human atrial myocytes using the baseline model (RA model). Time courses of (A) AP; (B) CaT; (C) active force; the data were normalised to the maximum value under the WT conditions, and (D) SL shortening. (E) Bar plots showing the peak active force relative to the WT case in various mutation conditions.

shortening was markedly decreased by 39.4% for D322H, 26.4% for E48G and 41.1% for A305T (Fig. 1Di).

On the other hand, the loss-of-function mutations prolonged AP duration, and increased the amplitude CaT, leading to an increased active force by 10.7%, 9.4% and 19.0% for Y155C, D469E and P488S, respectively (Fig. 1Cii), which was translated into a profound increase in the maximum SL shortening by 27.5%, 24.1% and 50.4% accordingly (Fig. 1Dii).

Quantitative reduction of the maximal active force by the gain-of-function mutations (D322H, E48G and A305T) and increase of the maximal active force by the loss-of-function mutations (Y155C, D469E and P488S) relative to WT are shown in Fig. 1Ei & Eii respectively.

In addition to simulations performed in sinus rhythm, the impact of the mutations on atrial contractility in the presence of AF-induced ionic remodelling was also assessed (Supplement Fig. 2). The results showed that whilst the impacts of the mutations on the APD, CaT, force and SL shortening under the AF-remodelled conditions were consistent with those under the sinus rhythm conditions (the gain- and loss-of-function mutations resulted in reduced and enhanced contractility, respectively, as compared to the WT), atrial contractility was markedly weaker for all mutations with AF-remodelling compared with the WT in the sinus rhythm.

In the absence of I_{SAC} (Supplement Fig. 3), simulation results were similar to those in the presence of I_{SAC}: the gain-of-function mutations reduced contractility, whereas the loss-of-function mutations mediated positive inotropic effects.

Similar inotropic consequences of the mutations seen in the baseline model (RA model) were also observed in other cell types (Fig. 2). In Fig. 2, effects of D322H (the most pronounced gain-of-function KCNA5 mutation) and P488S (the most severe loss-of-function mutation) on the electro-mechanical activity of various atrial cell types are compared with those in the WT conditions. It was shown that different atrial cell types exhibited pronounced AP heterogeneity (Fig. 2Ai), accompanied by noticeable differences in CaT (Fig. 2Bi), active force (Fig. 2Ci) and SL shortening (Fig. 2Di). The CT and BB cells exhibited greater contractility than the cells from the rest of the regions, due to a significantly higher CaT. PV and AS cells elicited more depolarised resting potential compared with other cell types. Such inter-regional heterogeneity though was reduced, but preserved by the gain-of-function D322H mutation (Fig. 2Aii–Dii), and augmented by the loss-of-function P488S mutation (Fig. 2Aiii–Diii).

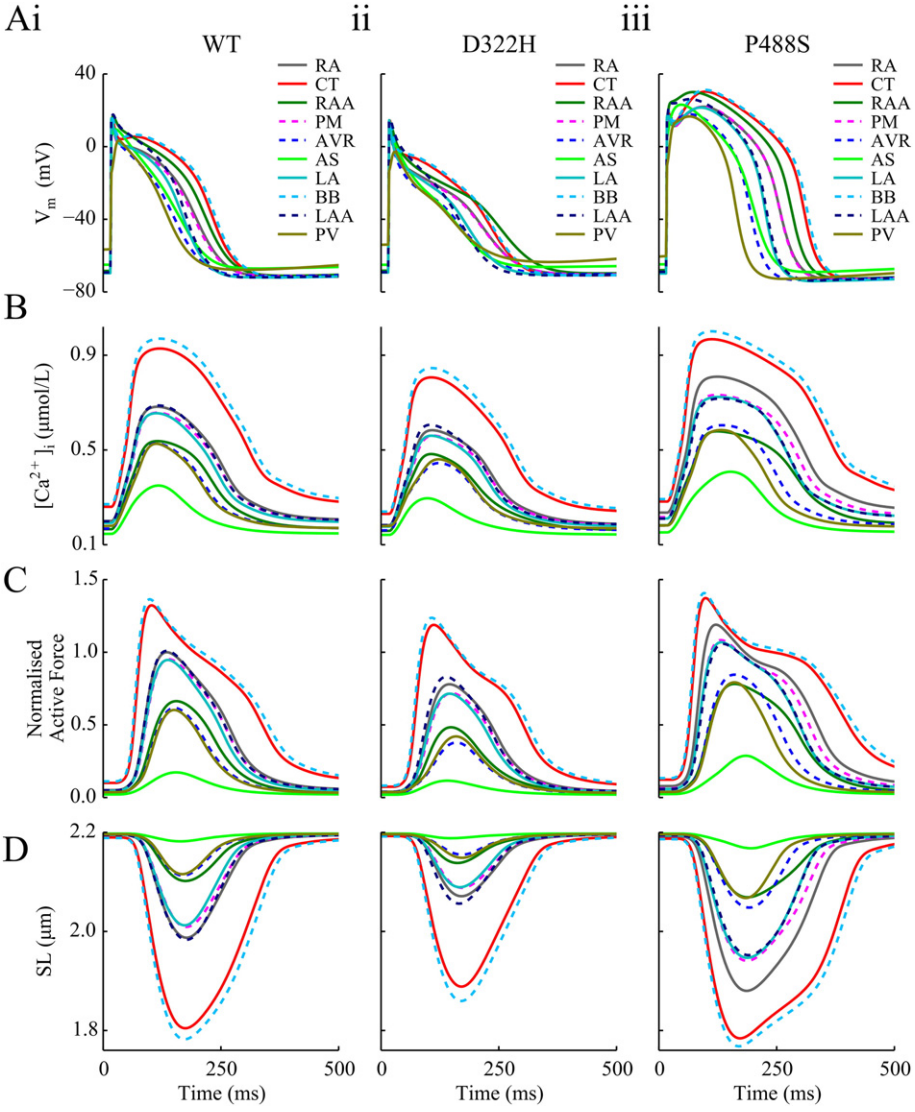

Fig. 2. Heterogeneous electro-mechanical activities in the isolated regional atrial cells for the WT (column i), D322H (column ii) and P488S (column iii). The panels show the time course of (Ai–Aiii) AP, (Bi–Biii) CaT, (Ci–Ciii) normalised active force and (Di–Diii) SL shortening. CT - crista terminalis, BB - Bachmann's bundle, PM - pectinate muscles, AVR - atrio-ventricular ring, RAA - right atrial appendage, AS - atrial septum, LA - left atrium, LAA - left atrial appendage, PV - pulmonary veins.

3.2. Mechanisms underlying the inotropic effects of the KCNA5 mutations

In order to elucidate the mechanism underlying inotropic effects of the KCNA5 mutations, we further analysed their functional effect on key ionic currents and the intracellular system regulating CaT that affects atrial mechanical dynamics, including the L-type calcium current (I_{CaL}), Na^+-Ca^{2+} exchanger (I_{NaCa}), ryanodine receptor (RyR) release flux (J_{rel}), sarcoplasmic reticulum (SR) uptake flux (J_{SERCA}) and SR content. Results are shown in Fig. 3 for the time courses (Fig. 3A–B) and time integrals (Fig. 3C–D) of I_{CaL} and I_{NaCa} elicited during APs. Current trances of I_{Kur}, the rapid and slow components of rectifier K^+ currents (I_{Kr} and I_{Ks}) and the fast Na^+ current (I_{Na}) are shown in Supplement Fig. 4.

For the gain-of-function mutations which depressed AP-plateau, although the peak amplitude of I_{CaL} was minimally increased as compared to the WT, the current was substantially smaller during the late phases of AP-repolarisation (Fig. 3Ai) due to hyperpolarised AP-plateau potential; the inward component of I_{NaCa} was increased during phase-2 and -3 of the AP (Fig. 3Bi), exhibiting an enhanced forward mode of the channel in favour of extruding Ca^{2+} out of the cell; consequently the uptake of Ca^{2+} to the SR was reduced, accompanied by a decreased Ca^{2+} release from the SR (Supplement Fig. 5Ai, Bi); a reduction was also seen in the resting SR content, despite that the systolic SR content during APs was not significantly affected by the mutations (Supplement Fig. 5Ci).

For the loss-of-function mutations, prolonged AP duration and altered AP profile produced a slight decrease in the I_{CaL} current during the plateau phase of AP (Fig. 3Aii) (more pronounced for P488S; these data are consistent with a previous study of blocking I_{Kur} in canine atrial cells [2]), but an increase during the late phases of the AP (Fig. 3Aii). These mutations also led to an increased outward component of the I_{NaCa} during the plateau and early phase-3 of AP (Fig. 3Bii), showing

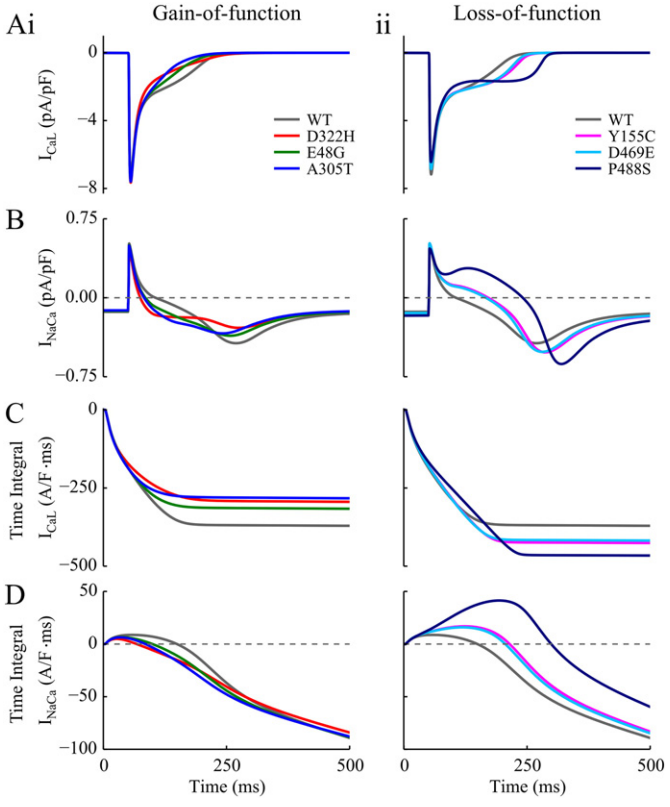

Fig. 3. Simulated time courses and time integrals of L-type Ca^{2+} current (I_{CaL}) and the Na^+-Ca^{2+} exchanger current (I_{NaCa}). (A) Time course of I_{CaL}. (B) Time course of I_{NaCa}. (C) Time integral of I_{CaL}. (D) Time integral of I_{NaCa}. Note that in panels (C) and (D), the time integrals were integrated from the time applying a current clamp evoking AP.

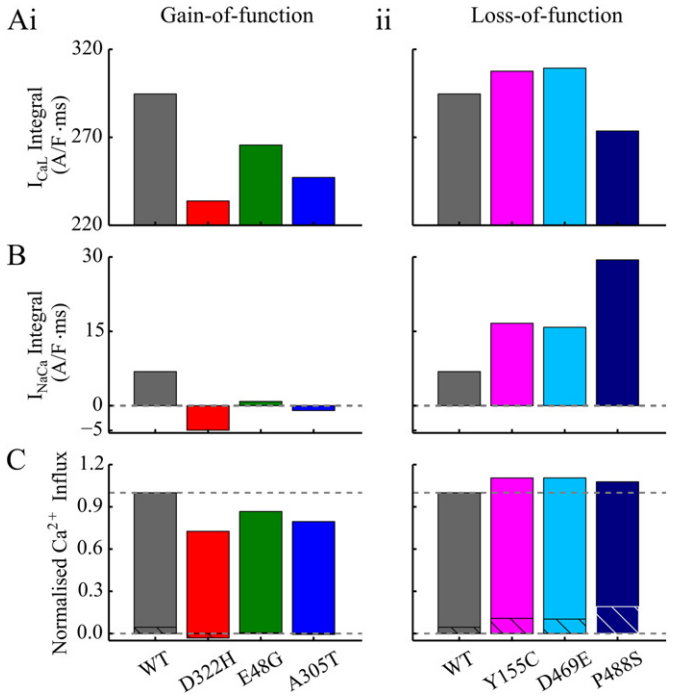

Fig. 4. The individual contribution of I_{CaL} and I_{NaCa} to the systolic CaT in the atrial cells for the WT and mutations. (A) The time integral of I_{CaL} at the peaking time of CaT. (B) The time integral of I_{NaCa} at the peak time of CaT. (C) Relative total Ca^{2+} entry contributing to the systolic CaT, which was calculated as $\int -I_{CaL}dt + 2 \cdot \int I_{NaCa}dt$ and normalised to the value of WT; specially, the contribution of I_{NaCa} to the Ca^{2+} entry preceding the peak of CaT was shown in hatched shadings.

an enhanced reversed mode of the exchanger that was in favour of Ca^{2+} import. The RyR and SERCA Ca^{2+} fluxes (Supplement Fig. 5A–Bii) were significantly increased by the mutations, and so were the resting SR levels (Supplement Fig. 5Cii).

The time integral of I_{CaL}, I_{NaCa}, J_{Rel} and J_{SERCA} during the time course of an AP, under various conditions were obtained through numerical integration. It was demonstrated that the time integral of I_{CaL} elicited by the AP was markedly reduced for the gain-of-function mutations vs. WT (Fig. 3Ci) due to shortened AP-plateau duration, resulting in smaller Ca^{2+} entries through the channel. In addition, the integral of I_{NaCa} manifested slightly increased activities of the exchanger working in the forward mode (Fig. 3Di); the integrals of RyR and SERCA activities were both reduced by the gain-of-function mutations (Supplement Figure 6Ai, Bi).

For the loss-of-function mutations, the integral of I_{CaL} was slightly (more noticeably for P488S) reduced for early repolarisation phases of AP, and was significantly increased in the later phases of AP (Fig. 3Cii); the integral of I_{NaCa} shows a consistently and significantly enhanced reversed mode dominated the exchanger throughout the AP repolarisation, which could directly contribute to the increased systolic CaT (Fig. 3Dii); the time integrals of the Ca^{2+} fluxes released from and uptake into the SR were both augmented (Supplement Fig. 6Aii, Bii).

To reveal the individual contribution of the altered I_{CaL} and I_{NaCa} arising from the secondary effect of the mutations to the systolic CaT, the time integrals of the two currents ($\int -I_{CaL}dt$ and $\int I_{NaCa}dt$) at the peak time of the CaT are illustrated in Fig. 4.

A marked reduction in the time integral of I_{CaL} until the peak time of CaT was observed for the gain-of-function mutations: the value was 294.6, 233.8, 265.6 and 247.2 A/F ·ms for WT, D322H, E48G and A305T respectively (Fig. 4Ai). The time integrals of I_{NaCa} until the peak of CaT were 6.9, −4.9, 0.8, −1.0 A/F·ms for WT, D322H, E48G and A305T, respectively (Fig. 4Bi).

The time integral of I_{CaL} until peak of CaT was also altered by the loss-of-function mutations: Y155C and D469E slightly increased the integral,

whereas it was reduced by the mutant P488S for which I_{Kur} was almost abolished (the values were 307.6, 309.3 and 273.6 A/F·ms for Y155C, D469E and P488S respectively, Fig. 4Aii). The time integral of I_{NaCa} until peak of CaT for the mutations as compared to the WT was increased: the integral was 16.6, 15.8 and 29.4 A/F·ms for Y155C, D469E and P488S, respectively (Fig. 4Bii).

The total Ca^{2+} entry through the two currents following the evoking of an AP until the peak time of CaT was quantified. The total Ca^{2+} entry contributing to the systolic CaT was calculated as $\int -I_{CaL}dt + 2\int I_{NaCa}dt$ and normalised to the value of WT (Fig. 4C). In comparison with the WT, the total Ca^{2+} entry until the peak time of CaT was significantly reduced by the gain-of-function mutations (by 27.4%, 13.3% and 20.5% for D322H, E48G and A305T, respectively, Fig. 4Ci), while it was increased by the loss-of-function mutations (by 10.5%, 10.6% and 7.8% for Y155C, D469E and P488S, respectively, Fig. 4Cii).

Furthermore, the relative contribution of I_{NaCa} to the total Ca^{2+} entry preceding the peak of CaT was also affected by the mutations (Fig. 4C): for WT 4.5% of Ca^{2+} entered the cytosol through the exchanger preceding the peak of CaT, whereas the values were −4.4% (a negative value indicates that the forward mode dominates the exchanger), around 0.1% and −0.1% for D322H, E48G and A305T, respectively. For the loss-of-function mutations, the relative contributions were 9.8%, 9.3% and 17.7% for Y155C, D469E and P488S, respectively. As a result, of the change in the amount of Ca^{2+} entry preceding the peak of CaT observed in the gain-of-function mutations, a fraction of 28.0%, 29.4% and 24.9% was attributed to the increased forward mode of I_{NaCa} for D322H, E48G and A305T, respectively; whereas the same metric was measured to be 60.1%, 54.9% and 187.6% for Y155C, D469E and P488S, respectively.

Therefore, the reduction of Ca^{2+} entry seen in the gain-of-function mutations were dominated by the decrease in I_{CaL}, whereas the enhanced reverse mode of I_{NaCa} played a more pronounced role in the increased Ca^{2+} entry by the loss-of-function mutations, exerting different inotropic effects of the two groups of the KCNA5 mutations on atrial cells.

3.3. Dependence of atrial contractility on I_{Kur} properties

The identified six KCN5A mutations caused a wide range of changes in the channel properties of I_{Kur}, including shifted activation curve and altered maximal channel conductance. In order to obtain a general picture of the dependence of atrial contractility on the properties of I_{Kur}, simulations were performed to quantify the relative cell shortenings with respect to varying parameters in the channel conductance and steady-state activation of I_{Kur}. Results are shown in Fig. 5.

It was shown that a positive shift in the $V_{1/2}$ (resulting in reduced I_{Kur}) of I_{Kur} activation curve resulted in an increase in the maximum relative cell shortening of the atrial cells: the relative cell shortening was 8.1%, 9.6% and 10.9% for $V_{1/2} = -11.0$, −6.0 and −1.0 mV, respectively.

In Fig. 5A–B, compared with the control parameters, a reduction in the channel conductance of I_{Kur} led to a significant increase (adding up to a further 7% to the relative cell shortening) in the cell contractility, whereas the augmented current densities exerted markedly blunted cell shortenings; a steeper steady-state activation curve ($K_{Activation}$ scaled by 0.2–0.8 fold) in I_{Kur} contributed to an increased cell shortening, whilst shallower steady-state activations (greater $K_{Activation}$ values) were associated with negative inotropic effects. Slightly decreased cell shortenings were observed for the simulations with slower kinetics (thus greater time constants) for the activation gate of I_{Kur} (Fig. 5Bi–iii).

In Fig. 5C, $K_{Activation}$ and $\tau_{Activation}$ were varied while the conductance was kept the same as control. Consistent-negative inotropic effects were demonstrated for slower kinetics in the activation/deactivation of I_{Kur}. The effects of varying $K_{Activation}$ within the parameter space were shown to be dependent on the $V_{1/2}$: for positively shifted $V_{1/2}$ shallower $K_{Activation}$ reduced the contractility of atrial cells, while both an increase and decrease in $K_{Activation}$ from its control value could lead to increased cell shortenings for the $V_{1/2}$ at the control or left-shifted values. Nevertheless, it should be noted that this nonlinearly dependent effect was relatively small in comparison with those when varying the conductance.

3.4. Inotropic effects of the KCNA5 mutations at the organ level

Due to the complex anatomical structure and intercellular electronic coupling in human atrial tissue, results obtained at the cellular level may not be extrapolated to the 3D organ level. Therefore, the inotropic effects of the KCNA5 mutations were further investigated by using a 3D anatomically accurate electro-mechanical model of human atria, which were paced at 1 Hz from the sinoatrial node (SAN) region.

Fig. 6 illustrates snapshots of simulated atrial electromechanical contraction for WT, D322H (the most pronounced gain-of-function mutation) and P488S (the most severe loss-of-function mutation), during a time course of 600 ms period, as well as the corresponding time course of the change in atrial volume. To illustrate the deformations of the tissue during contraction, an undeformed atrial mesh representing resting atria was superimposed and shown as a reference frame. The time courses of the dynamic electromechanical activities of the atria for WT, D322H and P488S can be seen in Online Supplementary Videos 1–3, respectively.

Snapshots at 10 ms (Fig. 6, top row) show that the excitation wave spread out from the SAN regions in the atria under the WT and mutation conditions. At 100 ms (second row), a majority of the atria was electrically activated for both WT and mutation conditions. At 200 ms (third row), a significant atrial contraction was observed for WT, which was more and less pronounced for P488S and D322H, respectively. The atrial deformations peaked between 200 and 250 ms (fourth row). At 300 ms the atria relaxation was underway for WT but was nearly completed for D322H whilst the relaxation just took place for P488S (fifth row). At 600 ms (sixth row) fully electrically and mechanically recovered atria were seen for all phenotypes.

The simulated time courses of computed atrial volume show that the amplitude of volume change and time span of contraction were reduced by the gain-of-function mutations, whereas they were increased by the loss-of-function mutations as compared to the WT condition. The observed differences in the atrial electrical and mechanical activation-relaxation intervals between the WT and mutation conditions were attributable to the alterations to the APD and CaT by the respective mutations observed at the single cell level.

We further quantified the effect of KCN5A mutations on atrial mechanical contraction. Results are shown in Fig. 7 for normalised atrial emptying volume (Fig. 7A) and peak atrial emptying rate (Fig. 7B) within a single simulated cardiac cycle. The atrial output was markedly reduced by the gain-of-function mutations in KCNA5 whereas it was significantly increased by the loss-of-function mutations. The relative decrease in emptying volume compared with the WT conditions were 37.2%, 24.1% and 37.5% for D322H, E48G and A305T, respectively, whereas a 24.4%, 21.4% and 42.6% increase in the atrial emptying volume were observed in the simulations with the loss-of-function mutations (for Y155C, D469E and P488S, respectively).

The rate of volume emptying was computed as an indicator for the atrial contraction velocity, as shown in Fig. 7B. The peak emptying rate was defined as $dV_{emptying}/dt|_{max}$, where $V_{emptying}$ is the atrial emptying volume. It was shown that complementary to the changes to the emptying volume, the peak volume emptying rate was also altered by the mutations. In comparison to the WT, the gain-of-function mutations induced a pronounced slowing down in peak rate of atrial contraction (by 38.1%, 24.5% and 35.5% for D322H, E48G and A305T, respectively). The same metric was increased by the loss-of-function mutations and the percentages were 26.8%, 18.0% and 39.7% for Y155C, D469E and P488S, respectively.

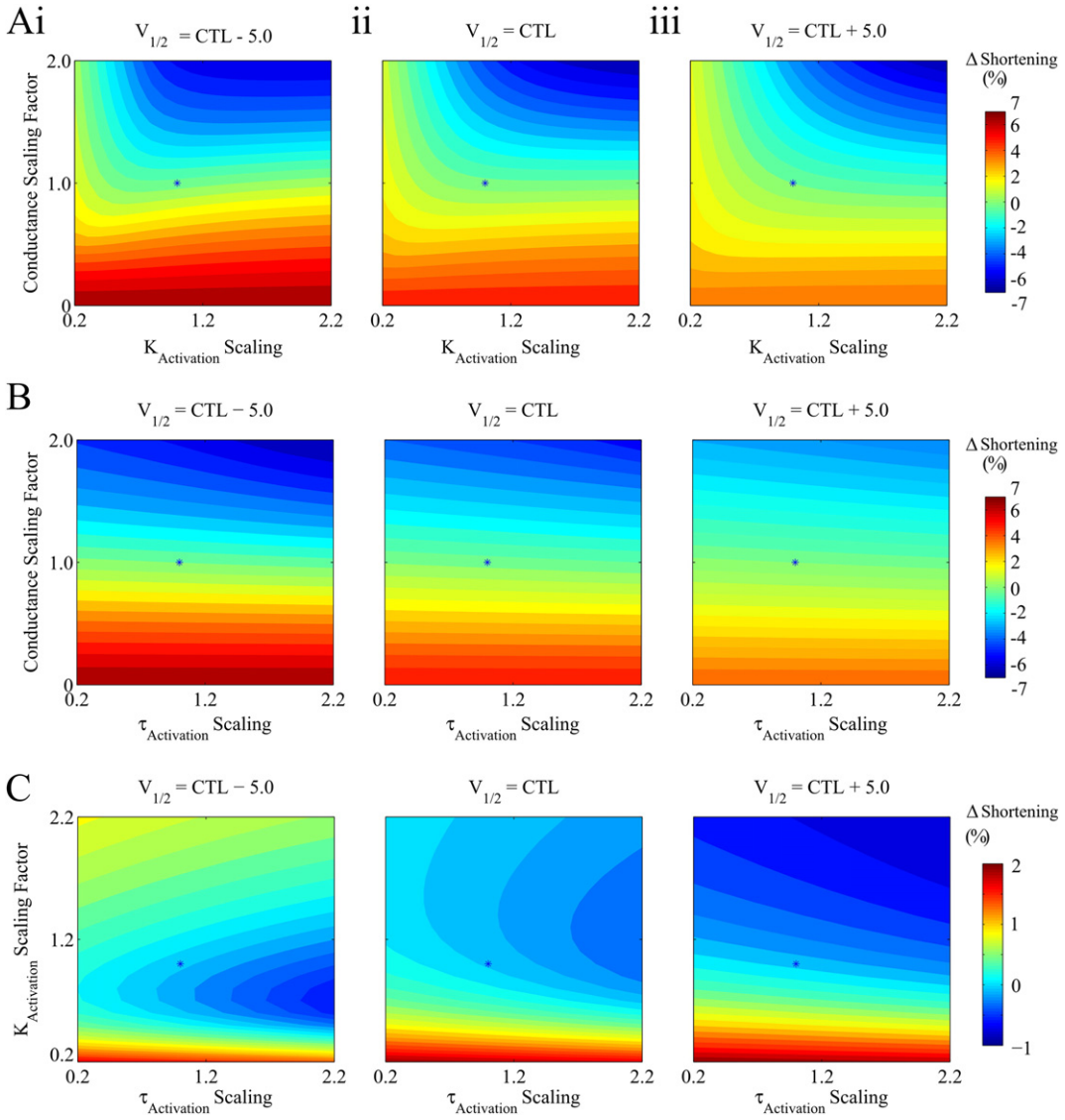

Fig. 5. The simulated dependence of relative cell shortening on the biophysical parameters of I_{Kur}. The dependence of the relative cell shortening to (A) varying conductance and $K_{Activation}$; (B) varying conductance and $\tau_{Activation}$; (C) varying $K_{Activation}$and $\tau_{Activation}$. In columns (i–iii) of each row, the $V_{1/2}$ of steady-state activation was shifted as labelled. In each panel, the difference in cell contractility was quantified as the change in relative cell shortening with respect to the relative cell shortening with parameters of interest at the control values (both assigned to 1.0, labelled with * in each panel).

Collectively, the gain-of-function mutations impaired the atrial contractile functions by reducing atrial emptying volume, attenuating the time span of contraction and slowing the atrial volume emptying rate. In contrast, the loss-of-function mutations increased atrial emptying volume accompanied by an accelerated emptying rate and prolonged atrial contraction duration.

4. Discussion

In this study, we developed a family of single cell models for human atrial electro-mechanics as well as a 3D anatomical model of atrial electromechanical coupling for WT and six KCN5A gene mutations identified in familial lone-AF patients [6]. These models were used to assess the functional impact of KCNA5 mutations on the contractile functions of human atria at both cellular and organ level in sinus rhythm. Possible underlying mechanisms responsible for the inotropic effects of the mutant I_{Kur} channels, especially the difference between the gain- and loss-of-function mutations were elucidated. The major contributions of this study are: (i) a new family of electromechanical models at cellular and 3D anatomical levels for control and KCN5A variants; (ii) elucidating that KCN5A mutations though impairing I_{Kur}, affect atrial mechanical contraction dynamics through their secondary effects on profiles of AP and CaT; (iii) revealing the two groups of KCN5A gene mutations exhibit distinctive inotropic effects: while the gain-of-function mutations reduced atrial contractility, the loss-of-function mutation enhanced atrial contractility; (iv) clarifying the mechanisms underlying the inotropic effects of the two mutation groups are different, which are discussed below.

4.1. Mechanistic insights to the inotropic effects of the KCNA5 mutations

4.1.1. Gain-of-function mutations

Gain-of-function mutations of I_{Kur} demonstrated negative inotropic effects at both the cellular and organ levels. At the single cell level, the mutations led to increased I_{Kur} current density, producing accelerated repolarisation in phase-1 and -2 of AP (Fig. 1, [7]). This was accompanied by a marked reduction in the CaT, leading to a significantly reduced active force production and hence markedly decreased relative cell shortening. Such changes at the cellular level were reflected at the organ level, which manifested as significantly smaller deformations in

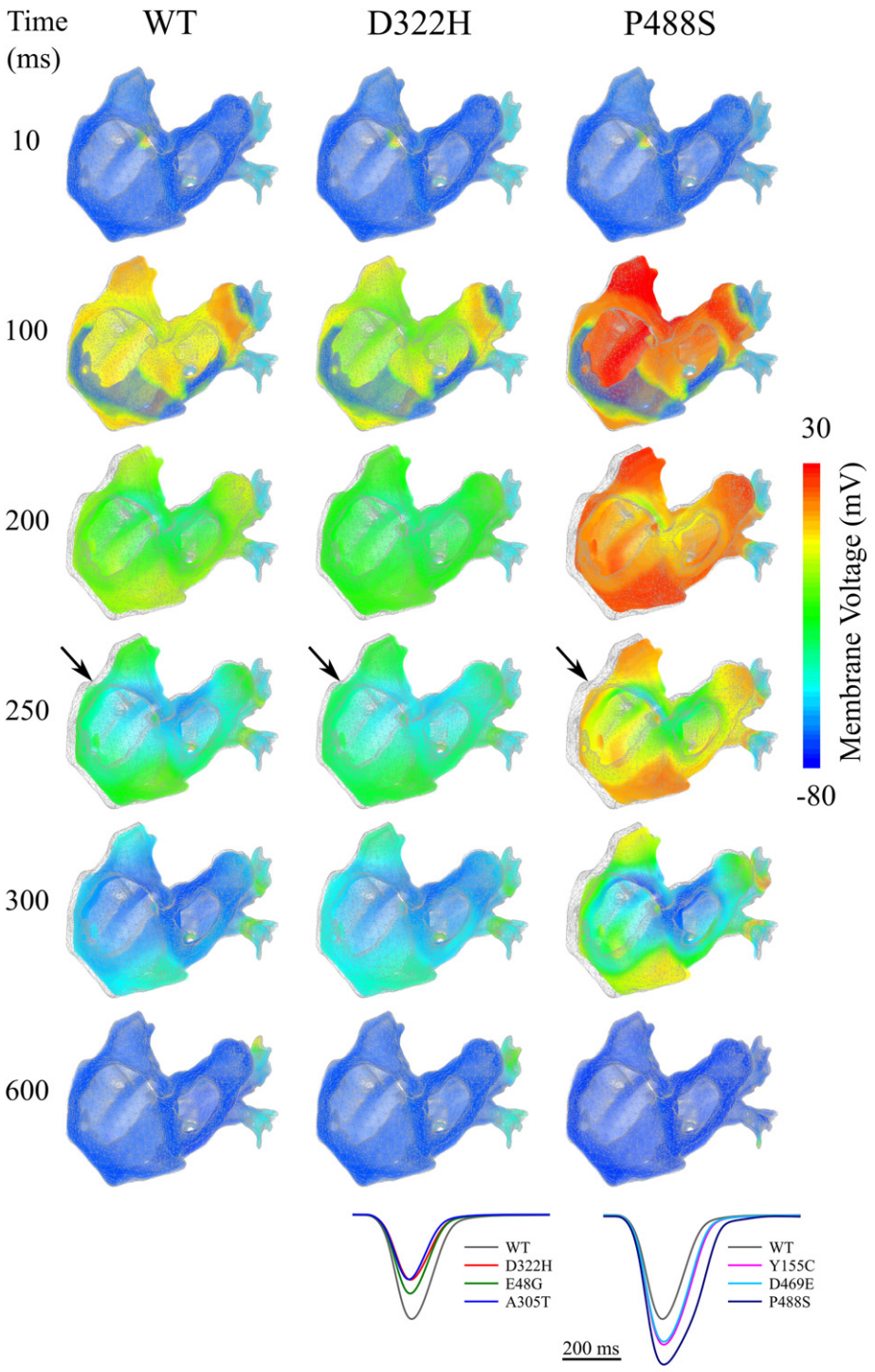

Fig. 6. Snapshots of simulated atrial electromechanical contraction and electrical excitation superimposed on the undeformed atrial mesh (in grey indicated with arrows) under the WT, D322H and P488S conditions. The simulated time following the application of an external stimulation from the SAN region is labelled in the left of the panels. Insert: time course of computed atrial volume.

the atrial myocardium (Fig. 6), notable reductions in the atrial empty volume (Fig. 7) and decelerated atrial emptying rates, as well as shortened time span of atrial contraction, demonstrating impaired atrial contractile functions.

The mechanism underlying the impaired atrial contractility by the gain-of-function mutations was elucidated. It was shown that altered AP profile by these mutations produced secondary actions, leading to a decreased Ca^{2+} entry through I_{CaL} and an enhanced Ca^{2+} export via I_{NaCa} working in the enhanced forward mode. Consequently, the amount of Ca^{2+} contributing to trigger the activation of RyR was reduced. The alterations to these two major currents facilitating the Ca^{2+} entry and export also resulted in a reduction in the SR content as a secondary effect, reducing the Ca^{2+} release flux from the SR through the RyR to the cytosol. Collectively, these mutations resulted in reduced Ca^{2+} induced Ca^{2+} release (CICR) in atrial myocytes. The quantifications in the time integral of I_{CaL} and I_{NaCa} indicated that the reduction in I_{CaL} dominated the reduction of the net Ca^{2+} entry that contributed to the reduced systolic CaT.

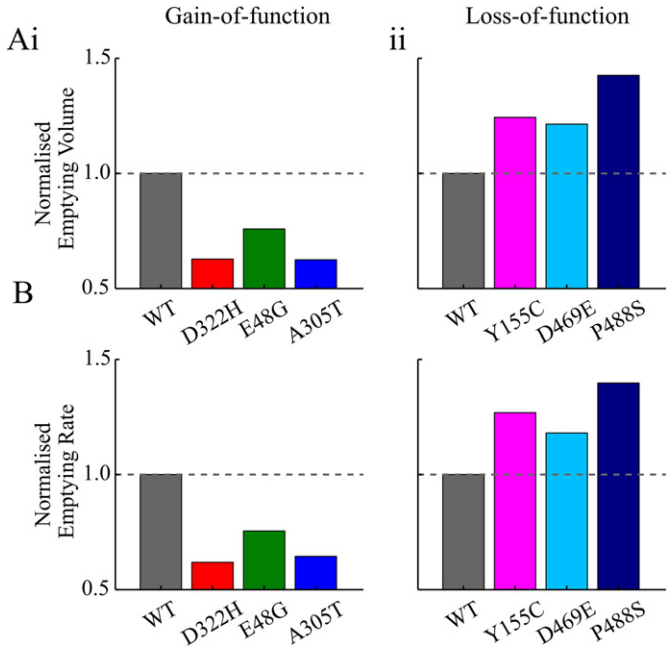

Fig. 7. Comparisons of atrial empty volume and peak emptying rate with respect to the WT and the mutations. (A) Normalised atrial emptying volume. (B) Normalised peak volume emptying rate. The values are normalised to those under the WT conditions.

4.1.2. Loss-of-function mutations

In contrast, the loss-of-function mutations in KCNA5 mediated positive inotropic effects in the human atria.

At the cellular level, the augmented CaT by the mutations resulted in an increased active force for Y155C, D469E and P488S, respectively. At 3D level, stronger atrial contraction was observed for the mutations, manifested by greater tissue mechanical deformations, an increase in the atrial empty volume as well as a similar amount of increase in the peak emptying rate and an extension of the time span of atrial contraction.

The underlying mechanisms of the positive inotropic effect of the loss-of-function mutations are different to those seen in the gain-of-function mutations. In the loss-of-function mutations conditions, the mutant I_{Kur} also altered AP profiles, producing slowing down in atrial repolarisation leading to elevated AP-plateau. Such altered AP profile was accompanied by an increased net Ca^{2+} entry (until the peak of CaT) through I_{NaCa}. This resulted in an increased systolic CaT, as well as an elevated SR content, leading to enhanced CICR activity. The increased net Ca^{2+} entry was primarily attributed to the increased I_{NaCa} working in the reverse mode which is favourable for Ca^{2+} entry. Specifically for P488S, the time integral of I_{CaL} that could directly contribute to the systolic CaT was in fact reduced but was overwhelmed by the increased Ca^{2+} entry through I_{NaCa}.

AF is associated with reduced atrial contractility [23], which seemingly contradicts with the positive inotropic effects of the loss-of-function mutations in sinus rhythm. To clarify and compare the inotropic effects of the mutation in the presence of AF-induced ionic remodelling, further simulations were performed by incorporating AF-remodelling parameters as used in our previous study [7]. Indeed, as compared to the WT in sinus rhythm, all genotypes resulted in markedly reduced contractility in AF-remodelled conditions (Supplement Fig. 2), suggesting that the AF-induced remodelling dominated the modulation of atrial contractility in persistent AF with both of the gain-of and loss-of-function mutations.

4.2. Parameter analysis of role of I_{Kur} in atrial contractility

So far several mutations have been identified in genes encoding I_{Kur} channels [4,6], each of which caused different alterations to the property and kinetics of the channel. By varying biophysical parameters of I_{Kur}, our data showed that the conductance, slope and $V_{1/2}$ of steady-state activation curve and kinetics of the activation gate of I_{Kur} play important roles in atrial contractility: an increased conductance, shallower steady-state activation curve, left shifted activation-voltage relation and slower activation/deactivation kinetics are in general associated with compromised atrial contractility. Among these parameters, the conductance dominated the modulations of the current on the active contraction of atrial myocytes.

4.3. Relevance to previous studies and clinical relevance

A family of electromechanical models incorporating regional electrical heterogeneities in the present study was based on the Colman et al. model of human atrial cells [7] and the Adeniran et al. model of atrial electromechanics [16]. Although electromechanical models have been extensively developed for ventricles [13,15,24–27], multi-scale models of atrial electromechanics is relatively rare [14]. The present study incorporates the inotropic effects of the KCNA5 mutations in 3D atrial electromechanical model.

The functional role of I_{Kur} in atrial electrical excitations has been investigated in previous studies [28–31]. Effects of I_{Kur} block on atrial contraction have been investigated experimentally both at cellular and organ level [2,32]. It is noteworthy that our simulated positive inotropic effects are concordant with previous experimental studies on effects of I_{Kur} block in the atria [2]. Following applications of AVE0118, an I_{to}/I_{Kur} blocker, profound increases in the atrial contractility were observed in the atria of goats [32], dogs, and humans [2]. In the study using atrial myocytes from human and canine hearts, Schotten et al. [2] revealed the enhanced atrial contractility seen following I_{Kur}/I_{to} block was attributable to a promoted Ca^{2+} entry via the reverse mode of I_{NaCa}. In the present study, the simulations suggest that loss-of-function mutations in I_{Kur} produced positive inotropic effects through a similar mechanism. Aligned with the experimental data [2,32], our modelling data support that I_{Kur} block is a potentially valuable strategy in the effort to enhance atrial contractility, which is desirable for the treatment of AF – especially following cardioversion of AF.

In contrast, the impact of gain-of-function in I_{Kur} on atrial mechanical function has not been well understood. The present study reveals that gain-of-function in I_{Kur} resulted in a reduced atrial active force and atrial output, and a decelerated volume emptying rate. At rest, the contraction of the atria contributes to approximately 20–30% of stroke volume in the left ventricle [11,33]. A reduction in atrial contraction may induce decreased ventricle outputs. Note that impaired atrial contraction has also been associated with AF [34]. The slowing down in atrial volume emptying rates in sinus rhythm may be linked with decelerated atrial wall contraction and hence slower blood flow in the upper chambers of the heart, which may be in favour of blood stasis and thus formation of new thrombi as occurred in AF [35].

In an in silico study published recently [7], we have investigated the pro-arrhythmogenesis of and especially the similarity and difference between the two different KCNA5 mutation groups. We demonstrated that the arrhythmogenicity of the KCNA5 mutations are distinct between the gain- and loss-of-function groups: the gain-of-function resulted in a shortened action potential duration and therefore a shortened excitation wavelength, facilitating the genesis and sustenance of re-entry; however, the loss-of-function mutations increased the vulnerability of tissue to early afterdepolarisations under the effect of beta-adrenergic stimulation, causing conduction block leading to formation of re-entry. The present study goes beyond the previous study, with a focus on the effects of the two groups of mutations on atrial contractility. Our results add insights into the functional impacts of the KCNA5 mutations on atrial electrical and mechanical dynamics, providing further understanding into how the mutations impair atrial electrical and mechanical properties including the spatial heterogeneity. The present study highlights the role of genetic mutations in potassium

channels in modulations of atrial contractility and represents, to the best of the author's knowledge, the first attempt to investigate such modulations using biophysically detailed and anatomically accurate multi-scale models.

4.4. Limitations

The limitations of the single cell model of atrial electromechanics [16] and 3D atrial model [14] have been discussed in detail in previous studies. Hence, only limitations specific to the present study are discussed here.

In this study, inotropic effects of KCNA5 mutations were compared with WT. It was assumed that these mutations did not mediate any changes other than alterations to I_{Kur} alone, i.e. the contraction apparatus of the myocytes, the electrical coupling in tissue, mechanical properties and atrial structure were not affected by the mutations. The validity of such assumptions necessitates further experimental investigations.

Another limitation is that these effects were considered in sinus rhythm. The impaired atrial contractility by AF is also associated with fast excitation rates seen in AF, which will certainly affect the effects of the gain- and loss-of-function mutations on atrial mechanical dynamics. However, incorporating the effects of excitation rates may increase the complication of the results, which may obscure the data interpretation. As the focus of the present study was to compare and clarify the different effects of the two mutation groups on atrial contractility, we only considered the sinus rhythm condition.

MEF was incorporated by the inclusion of a non-selective stretch-activated channel following previous simulations [13,26,36]. Other effects introduced by MEF such as stretch-induced changes to the intracellular Ca^{2+} handling system [37] and modulation of the AP through alterations to the coupled cardiac fibroblasts [38,39] were not considered. The impact of incorporating such effects together with the role of the interplay between the mutations and I_{SAC} in the arrhythmogenicity of these mutations may warrant further investigations.

5. Conclusion

The present study highlights an important role of I_{Kur} in modulating human atrial contractility. The gain-of-function KCNA5 mutations resulted in a profound impairment to atrial contractility, primarily through reducing the Ca^{2+} entry via I_{CaL}. The loss-of-function KCNA5 mutations mediated positive inotropic effects though promoting the Ca^{2+} entry via increased reverse mode of I_{NaCa}. These findings add insights into the functional impacts of genetic variations in KCNA5 on human atrial contractility further to the modulations of the mutations on atrial electrical activities.

Supplementary data to this article can be found online at http://dx.doi.org/10.1016/j.yjmcc.2017.08.005.

Acknowledgement

This work was funded by EPSRC (UK) (EP/J00958X/1), BHF (FS/14/15/30533), the National Natural Science Foundation of China (61572152, 61571165) and MC-IRSES CORDIS3D (317766), Shenzhen Science and Technology Innovation Committee (JCYJ20151029173639477; JSGG20160229125049615). HN was supported by the Dean's Scholarship from the University of Manchester.

References

[1] E. Wettwer, O. Hála, T. Christ, J.F. Heubach, D. Dobrev, M. Knaut, A. Varró, U. Ravens, Role of IKur in controlling action potential shape and contractility in the human atrium influence of chronic atrial fibrillation, Circulation 110 (2004) 2299–2306, http://dx.doi.org/10.1161/01.CIR.0000145155.60288.71.

[2] U. Schotten, S. de Haan, S. Verheule, E.G.A. Harks, D. Frechen, E. Bodewig, M. Greiser, R. Ram, J. Maessen, M. Kelm, M. Allessie, D.R.V. Wagoner, Blockade of atrial-specific K+-currents increases atrial but not ventricular contractility by enhancing reverse mode Na+/Ca2+-exchange, Cardiovasc. Res. 73 (2007) 37–47, http://dx.doi.org/10.1016/j.cardiores.2006.11.024.

[3] M.C. Brandt, L. Priebe, T. Böhle, M. Südkamp, D.J. Beuckelmann, The ultrarapid and the transient outward K+ current in human atrial fibrillation. Their possible role in postoperative atrial fibrillation, J. Mol. Cell. Cardiol. 32 (2000) 1885–1896, http://dx.doi.org/10.1006/jmcc.2000.1221.

[4] T.M. Olson, A.E. Alekseev, X.K. Liu, S. Park, L.V. Zingman, M. Bienengraeber, S. Sattiraju, J.D. Ballew, A. Jahangir, A. Terzic, Kv1.5 channelopathy due to KCNA5 loss-of-function mutation causes human atrial fibrillation, Hum. Mol. Genet. 15 (2006) 2185–2191, http://dx.doi.org/10.1093/hmg/ddl143.

[5] S. Nattel, B. Burstein, D. Dobrev, Atrial remodeling and atrial fibrillation mechanisms and implications, Circ. Arrhythm. Electrophysiol. 1 (2008) 62–73, http://dx.doi.org/10.1161/CIRCEP.107.754564.

[6] I.E. Christophersen, M.S. Olesen, B. Liang, M.N. Andersen, A.P. Larsen, J.B. Nielsen, S. Haunsø, S.-P. Olesen, A. Tveit, J.H. Svendsen, N. Schmitt, Genetic variation in KCNA5: impact on the atrial-specific potassium current IKur in patients with lone atrial fibrillation, Eur. Heart J. 34 (2013) 1517–1525, http://dx.doi.org/10.1093/eurheartj/ehs442.

[7] M.A. Colman, H. Ni, B. Liang, N. Schmitt, H. Zhang, In silico assessment of genetic variation in KCNA5 reveals multiple mechanisms of human atrial arrhythmogenesis, PLoS Comput. Biol. 13 (2017) e1005587, http://dx.doi.org/10.1371/journal.pcbi.1005587.

[8] P. Samet, W.H. Bernstein, D.A. Nathan, A. López, Atrial contribution to cardiac output in complete heart block, Am. J. Cardiol. 16 (1965) 1–10, http://dx.doi.org/10.1016/0002-9149(65)90002-0.

[9] J. Mukharji, R.B. Rehr, A. Hastillo, J.A. Thompson, M.L. Hess, W.J. Paulsen, G.W. Vetrovec, Comparison of atrial contribution to cardiac hemodynamics in patients with normal and severely compromised cardiac function, Clin. Cardiol. 13 (1990) 639–643, http://dx.doi.org/10.1002/clc.4960130910.

[10] J. Hauser, I. Michel-Behnke, K. Zervan, C. Pees, Noninvasive measurement of atrial contribution to the cardiac output in children and adolescents with congenital complete atrioventricular block treated with dual-chamber pacemakers, Am. J. Cardiol. 107 (2011) 92–95, http://dx.doi.org/10.1016/j.amjcard.2010.08.050.

[11] I. Ovsyshcher, R. Zimlichman, A. Katz, C. Bondy, S. Furman, Measurements of cardiac output by impedance cardiography in pacemaker patients at rest: effects of various atrioventricular delays, J. Am. Coll. Cardiol. 21 (1993) 761–767.

[12] M.R. Franz, F. Bode, Mechano-electrical feedback underlying arrhythmias: the atrial fibrillation case, Prog. Biophys. Mol. Biol. 82 (2003) 163–174, http://dx.doi.org/10.1016/S0079-6107(03)00013-0.

[13] I. Adeniran, J.C. Hancox, H. Zhang, In silico investigation of the short QT syndrome, using human ventricle models incorporating electromechanical coupling, Front. Card. Electrophysiol. 4 (2013) 166, http://dx.doi.org/10.3389/fphys.2013.00166.

[14] I. Adeniran, D.H. MacIver, C.J. Garratt, J. Ye, J.C. Hancox, H. Zhang, Effects of persistent atrial fibrillation-induced electrical remodeling on atrial electro-mechanics – insights from a 3D model of the human atria, PLoS One 10 (2015) e0142397, http://dx.doi.org/10.1371/journal.pone.0142397.

[15] X. Jie, V. Gurev, N. Trayanova, Mechanisms of mechanically induced spontaneous arrhythmias in acute regional ischemia, Circ. Res. 106 (2010) 185–192, http://dx.doi.org/10.1161/CIRCRESAHA.109.210864.

[16] P. Brocklehurst, H. Ni, H. Zhang, J. Ye, Electro-mechanical dynamics of spiral waves in a discrete 2D model of human atrial tissue, PLoS One 12 (2017) e0176607, http://dx.doi.org/10.1371/journal.pone.0176607.

[17] J.J. Rice, F. Wang, D.M. Bers, P.P. de Tombe, Approximate model of cooperative activation and crossbridge cycling in cardiac muscle using ordinary differential equations, Biophys. J. 95 (2008) 2368–2390, http://dx.doi.org/10.1529/biophysj.107.119487.

[18] S. Fareh, C. Villemaire, S. Nattel, Importance of refractoriness heterogeneity in the enhanced vulnerability to atrial fibrillation induction caused by tachycardia-induced atrial electrical remodeling, Circulation 98 (1998) 2202–2209, http://dx.doi.org/10.1161/01.CIR.98.20.2202.

[19] J. Feng, L. Yue, Z. Wang, S. Nattel, Ionic mechanisms of regional action potential heterogeneity in the canine right atrium, Circ. Res. 83 (1998) 541–551, http://dx.doi.org/10.1161/01.RES.83.5.541.

[20] O.V. Aslanidi, M.A. Colman, J. Stott, H. Dobrzynski, M.R. Boyett, A.V. Holden, H. Zhang, 3D virtual human atria: a computational platform for studying clinical atrial fibrillation, Prog. Biophys. Mol. Biol. 107 (2011) 156–168, http://dx.doi.org/10.1016/j.pbiomolbio.2011.06.011.

[21] M.A. Colman, O.V. Aslanidi, S. Kharche, M.R. Boyett, C. Garratt, J.C. Hancox, H. Zhang, Pro-arrhythmogenic effects of atrial fibrillation-induced electrical remodelling: insights from the three-dimensional virtual human atria, J. Physiol. 591 (2013) 4249–4272, http://dx.doi.org/10.1113/jphysiol.2013.254987.

[22] G. Seemann, C. Höper, F.B. Sachse, O. Dössel, A.V. Holden, H. Zhang, Heterogeneous three-dimensional anatomical and electrophysiological model of human atria, Philos. Trans. R. Soc. Lond. Math. Phys. Eng. Sci. 364 (2006) 1465–1481, http://dx.doi.org/10.1098/rsta.2006.1781.

[23] U. Schotten, J. Ausma, C. Stellbrink, I. Sabatschus, M. Vogel, D. Frechen, F. Schoendube, P. Hanrath, M.A. Allessie, Cellular mechanisms of depressed atrial contractility in patients with chronic atrial fibrillation, Circulation 103 (2001) 691–698, http://dx.doi.org/10.1161/01.CIR.103.5.691.

[24] I. Adeniran, J.C. Hancox, H. Zhang, Effect of cardiac ventricular mechanical contraction on the characteristics of the ECG: a simulation study, J. Biomed. Sci. Eng. 06 (2013) 47, http://dx.doi.org/10.4236/jbise.2013.612A007.

[25] I. Adeniran, D.H. MacIver, J.C. Hancox, H. Zhang, Abnormal calcium homeostasis in heart failure with preserved ejection fraction is related to both reduced contractile function and incomplete relaxation: an electromechanically detailed biophysical modeling study, Card. Electrophysiol. 6 (2015) 78, http://dx.doi.org/10.3389/fphys.2015.00078.

[26] L.D. Weise, A.V. Panfilov, A discrete electromechanical model for human cardiac tissue: effects of stretch-activated currents and stretch conditions on restitution properties and spiral wave dynamics, PLoS One 8 (2013) e59317, http://dx.doi.org/10.1371/journal.pone.0059317.
[27] R. Chabiniok, V.Y. Wang, M. Hadjicharalambous, L. Asner, J. Lee, M. Sermesant, E. Kuhl, A.A. Young, P. Moireau, M.P. Nash, D. Chapelle, D.A. Nordsletten, Multiphysics and multiscale modelling, data-model fusion and integration of organ physiology in the clinic: ventricular cardiac mechanics, Interface Focus 6 (2016) 20150083, http://dx.doi.org/10.1098/rsfs.2015.0083.
[28] J. Almquist, M. Wallman, I. Jacobson, M. Jirstrand, Modeling the effect of Kv1.5 block on the canine action potential, Biophys. J. 99 (2010) 2726–2736, http://dx.doi.org/10.1016/j.bpj.2010.08.062.
[29] E.P. Scholz, P. Carrillo-Bustamante, F. Fischer, M. Wilhelms, E. Zitron, O. Dössel, H.A. Katus, G. Seemann, Rotor termination is critically dependent on kinetic properties of IKur inhibitors in an in silico model of chronic atrial fibrillation, PLoS One 8 (2013) e83179, http://dx.doi.org/10.1371/journal.pone.0083179.
[30] K. Tsujimae, S. Murakami, Y. Kurachi, In silico study on the effects of IKur block kinetics on prolongation of human action potential after atrial fibrillation-induced electrical remodeling, Am. J. Physiol. Heart Circ. Physiol. 294 (2008) H793–H800, http://dx.doi.org/10.1152/ajpheart.01229.2007.
[31] Q. Zhou, G.C.L. Bett, R.L. Rasmusson, Markov models of use-dependence and reverse use-dependence during the mouse cardiac action potential, PLoS One 7 (2012) e42295, http://dx.doi.org/10.1371/journal.pone.0042295.
[32] S. de Haan, M. Greiser, E. Harks, Y. Blaauw, A. van Hunnik, S. Verheule, M. Allessie, U. Schotten, AVE0118, blocker of the transient outward current (Ito) and Ultrarapid delayed rectifier current (IKur), fully restores atrial contractility after cardioversion of atrial fibrillation in the goat, Circulation 114 (2006) 1234–1242, http://dx.doi.org/10.1161/CIRCULATIONAHA.106.630905.
[33] Y. Iwasaki, K. Nishida, T. Kato, S. Nattel, Atrial fibrillation pathophysiology, Circulation 124 (2011) 2264–2274, http://dx.doi.org/10.1161/CIRCULATIONAHA.111.019893.
[34] A.C. Boyd, N.B. Schiller, D.L. Ross, L. Thomas, Segmental atrial contraction in patients restored to sinus rhythm after cardioversion for chronic atrial fibrillation: a colour Doppler tissue imaging study, Eur. Heart J. Cardiovasc. Imaging. 9 (2008) 12–17, http://dx.doi.org/10.1016/j.euje.2006.11.004.
[35] J.J. Goldberger, R. Arora, D. Green, P. Greenland, D.C. Lee, D.M. Lloyd-Jones, M. Markl, J. Ng, S.J. Shah, Evaluating the atrial myopathy underlying atrial fibrillation identifying the arrhythmogenic and thrombogenic substrate, Circulation 132 (2015) 278–291, http://dx.doi.org/10.1161/CIRCULATIONAHA.115.016795.
[36] N.H.L. Kuijpers, H.M.M. ten Eikelder, P.H.M. Bovendeerd, S. Verheule, T. Arts, P.A.J. Hilbers, Mechanoelectric feedback leads to conduction slowing and block in acutely dilated atria: a modeling study of cardiac electromechanics, Am. J. Physiol. Heart Circ. Physiol. 292 (2007) H2832–H2853, http://dx.doi.org/10.1152/ajpheart.00923.2006.
[37] S.C. Calaghan, E. White, The role of calcium in the response of cardiac muscle to stretch, Prog. Biophys. Mol. Biol. 71 (1999) 59–90, http://dx.doi.org/10.1016/S0079-6107(98)00037-6.
[38] P. Kohl, P. Hunter, D. Noble, Stretch-induced changes in heart rate and rhythm: clinical observations, experiments and mathematical models, Prog. Biophys. Mol. Biol. 71 (1999) 91–138, http://dx.doi.org/10.1016/S0079-6107(98)00038-8.
[39] P. Kohl, D. Noble, Mechanosensitive connective tissue: potential influence on heart rhythm, Cardiovasc. Res. 32 (1996) 62–68.